Single-crystalline (100) Ge networks on insulators by rapid-melting growth along hexagonal mesh-pattern

Toko, Kaoru
Department of Electronics, Kyushu University

Ohta, Yasuharu
Department of Electronics, Kyushu University

Sakane, Takashi
Department of Electronics, Kyushu University

Sadoh, Taizoh
Department of Electronics, Kyushu University

他

KYUSHU UNIVERSITY

Single-crystalline (100) Ge networks on insulators by rapid-melting growth along hexagonal mesh-pattern

Kaoru Toko,[1,a)] Yasuharu Ohta,[1] Takashi Sakane,[1] Taizoh Sadoh,[1] Ichiro Mizushima,[2] and Masanobu Miyao[1,b)]

[1]*Department of Electronics, Kyushu University, 744 Motooka, Fukuoka 819-0395, Japan*
[2]*Semiconductor Technology Academic Research Center, 3-17-2 Shinyokohama, Yokohama 220-0033, Japan*

Single-crystalline-Ge (c-Ge) networks on insulator films formed on Si substrates are essential for integrating high-speed and multifunctional devices onto the Si-platform. Rapid-melting-growth of mesh-patterned amorphous-Ge is examined over large areas (500×250 μm^2). For squared-mesh-pattern, polycrystalline-Ge forms throughout most of the mesh, though c-Ge is obtained near (<100 μm) Si-seed. Based on the consideration of geometric-effects, mesh-patterns are changed to hexagonal. This realizes c-Ge networks over the entire insulator area. These results indicate that Ge growth initiated from Si-seed propagates laterally over the hexagonal-mesh-pattern though bending and branching. These unique c-Ge-networks on insulators facilitate Ge-based advanced-devices on the Si-platform. © *2011 American Institute of Physics.*
[doi:10.1063/1.3544057]

Single-crystalline-Ge (c-Ge) thin-films (<100 nm) on insulators (GOI) are essential structures for achieving advanced high-speed transistors with high carrier mobilities, low parasitic capacitances, and low junction leakage currents.[1–3] The oxidation-induced Ge condensation process[4,5] and wafer bonding techniques[6] have been developed. However, the former has low carrier mobility (410 cm^2/V s),[5] which is caused by oxidation-induced point-defects. In the latter, the fabrication process of the Ge thin films is complex.

Recently, seeded rapid-melting-growth of amorphous-Ge (a-Ge) has been investigated. This enabled the growth of defect-free single-crystalline (100) GOI strips that are 20–40 μm long and 2–3 μm wide.[7–10] The monolithic integration of GOI transistors with Si transistors on a Si substrate was also demonstrated.[11] Our efforts in the past several years have focused on the mechanism of this growth.[12] This has enabled the optimization of both sample structures and annealing conditions. As a result, giant (100), (110), and (111) GOI strips (>400 μm), which are over one order of magnitude longer than previously achieved.[12,13] Moreover, we demonstrated very high hole mobility (~ 1100 cm^2/V s),[13–15] which indicates high GOI crystal quality. These results have caused the expectation that high mobility Ge transistors will be integrated with Si large-scale integrated circuits.

However, formation of uniform and flat c-Ge strip arrays is difficult because of Ge aggregation during the melt-back process. This has limited the strip width to less than 5 μm. Consequently, Ge transistors must be fabricated on the narrow Ge strip arrays. This is an impediment to achieving high-density Ge transistor circuits. A possible solution to obtain large-area GOI is the formation of Ge networks composed of crossing strips, i.e., the mesh-pattern, which has not been studied yet.

This paper describes the seeded rapid-melting growth of Ge along these mesh-patterned structures. The influence of bending and branching during lateral growth specific for this structure are comprehensively studied. This enables c-Ge networks with a hexagonal mesh-pattern to cover a large area (500×250 μm^2).

In the experiments, Si (100) substrates (600 μm thickness) covered with Si$_3$N$_4$ films (100 nm thickness) were used. These films were patterned using wet etching to form seeding areas (50×300 μm^2). The edges of the seeding areas were formed perpendicular to the $\langle 011 \rangle$ direction. Subsequently, 100-nm-thick a-Ge layers were deposited using a molecular-beam epitaxy (MBE) system, with a base pressure of 5×10^{-10} Torr. They were patterned into a square mesh (Ge strip width: 3 μm and openings: 5×5 μm^2). The sample structure is schematically shown in Fig. 1(a). Then, an 800-nm-thick SiO$_2$ layer was deposited using RF-magnetron sputtering. Finally, these samples were heat-treated using pre-heating (800 °C, 1 min) followed by rapid
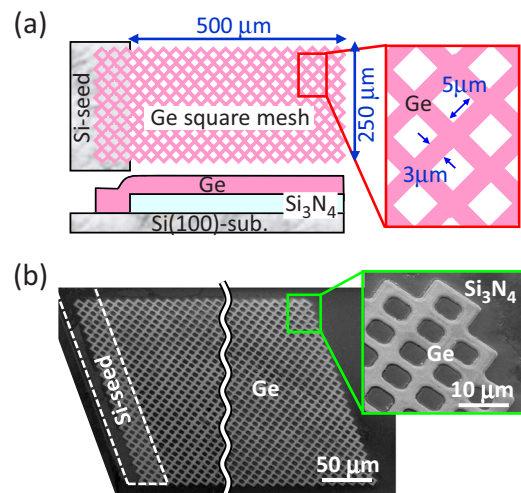

FIG. 1. (Color online) (a) Schematic sample structure with the square mesh-pattern. (b) SEM images of a GOI sample after RTA (1000 °C, 1 s).

a)Electronic mail: k_toko@nano.ed.kyushu-u.ac.jp.
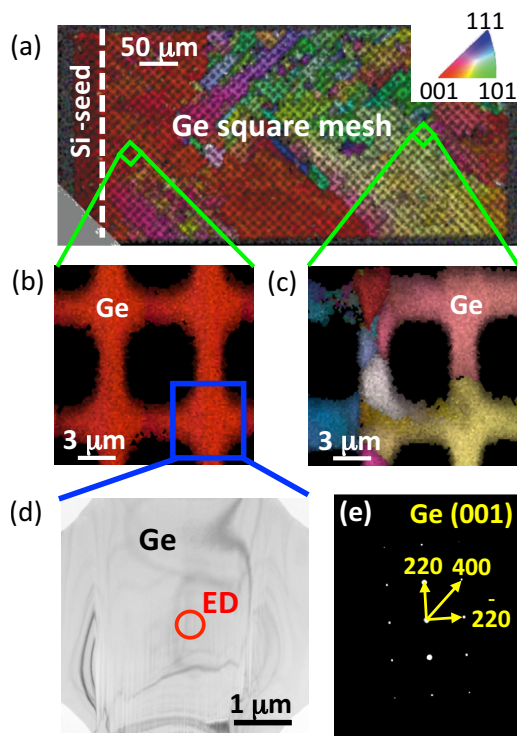b)Electronic mail: miyao@ed.kyushu-u.ac.jp.

FIG. 2. (Color online) (a) EBSD image of a GOI sample over the entire mesh-pattern region (500×250 μm^2). Magnified images (b) near and (c) far from the seeding region after RTA (1000 °C, 1 s). (d) TEM image and (e) ED pattern of a single-crystalline GOI sample at a crossing region of the mesh-pattern.
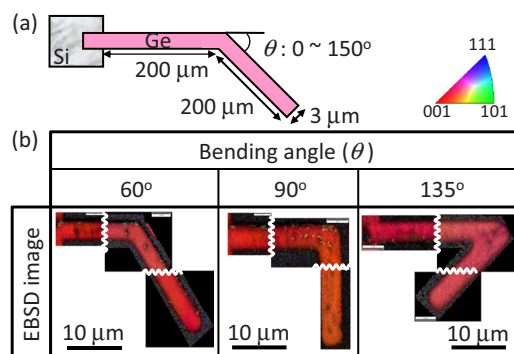

FIG. 3. (Color online) (a) Schematic sample structure of the Ge strip with a single-bending pattern. (b) EBSD images of annealed samples (1000 °C, 1 s) with bending angles of 60°, 90°, and 135°.

thermal annealing (RTA) at 1000 °C (1 s). This process was used to induce the melting growth from the seeding areas, i.e., from the Si substrate. The surface morphology, crystal orientation, and crystal quality of the grown layers were characterized using scanning electron microscopy (SEM), electron backscattering diffraction (EBSD), and plane-view transmission electron microscopy (TEM). The SiO$_2$ capping layers were removed before these measurements.

SEM images of the annealed sample are shown in Fig. 1(b), which show the uniform and flat Ge surface that lacks Ge aggregation. The crystal orientation map for the entire area obtained using the EBSD measurements is shown in Fig. 2(a). Magnified EBSD images of the Ge network both near and far from the Si-seed are shown in Figs. 2(b) and 2(c), respectively. These results indicate that Ge growth initiated from Si (100) seed propagates laterally along the mesh-patterned Ge. The lateral growth extends 100 μm from the Si-seed. However, significant changes in the Ge orientation occur for the regions far (>100 μm) from the Si-seed. This results in the formation of polycrystalline Ge, as shown in Fig. 2(c). Such phenomena will be discussed later.

Note that no grain boundaries are detected in the magnified EBSD image in Fig. 2(b), even though at least one collision of melting growth-front must exist in this area. Similar results were reported for the lateral vapor-phase epitaxy of Ge, where two fronts of lateral growths that were initiated from different positions on the same Si-substrate, collided on the SiO$_2$ without generating visible defects.[16,17] These results suggest that Ge melting-growth initiated from the Si-substrate propagates while maintaining its orientation perfectly, as reported for lateral vapor-phase epitaxy.[16,17] The

TEM images shown in Fig. 2(d) reveal no dislocation or stacking fault in the crossing region, even though strain-originated black lines are visible. In addition, the electron diffraction (ED) pattern shown in Fig. 2(e) exhibits clear spots of (100) Ge, indicating coherent lateral growth from the (100) Si-substrate. These results suggest that the crystal quality of the (100) GOI grown along mesh-pattern is as high as that of the straight strip-patterns reported in our previous work.[12–15]

Now, let us consider the polycrystallization phenomena shown in the region far (>100 μm) from the Si-seed [Fig. 2(c)], which have never been observed in lateral (100) Ge growth when using the straight strip-pattern. The mesh-pattern differs from the strip-pattern geometrically because of its existence of bending and branching during lateral growth. Consequently, influence of the bending during growth on the crystal quality is studied as a first step. Here, new strip-patterns with bending structures (total strip lengths: 400 μm, bending angles (θ): 60°, 90°, and 135°) are employed. This is shown in Fig. 3(a). EBSD images taken after annealing are shown in Fig. 3(b). These images clearly indicate that the lateral Ge growth for all samples propagates over 400 μm without a change in orientation. These results clearly indicate that bending of growth direction encountered in mesh-patterned growth is not the main reason for making polycrystalline Ge shown in Fig. 2(c).

The branching during lateral growth is another factor to be examined. Generally, melting growth generates latent heat at the solid-liquid interface, i.e., a growth-front, which flows into the solid-Ge region. When the lateral growth-front arrives at the branching-region, the number of solid-liquid interfaces increases. Consequently, the flux of heat-flow from liquid to solid Ge is increased through the branching, which decreases the cooling rate at the growth-front. This retarded melt-back growth at each branching region prolongs the melting-time in the liquid-Ge in regions far from the seed. This enhances the probability of random spontaneous nucleation, which results in polycrystallization. In Fig. 2(c), polycrystallization in a square mesh-pattern, where one growth-front branches into three at each crossing point, can be observed (branching number: 3). However, polycrystallization was not observed for (100) Ge growth along strip-pattern (branching number: 1).[12,13] Therefore, experiments with a branching number of two could be of special interest.

To study this, additional experiments using a hexagonal-type mesh-pattern (branching number: 2) are carried out. The
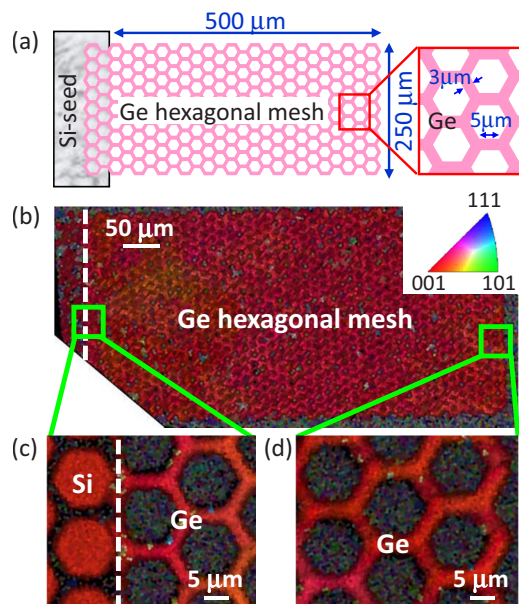
FIG. 4. (Color online) (a) Schematic sample structure with a hexagonal mesh-pattern. (b) EBSD image of a GOI sample over the entire mesh-region. Magnified images (c) near and (d) far from the Si-seed after RTA (1000 °C, 1 s).

sample structure is schematically shown in Fig. 4(a), and EBSD images taken after annealing are shown in Figs. 4(b)–4(d). These EBSD images show the crystal orientation over the entire region [Fig. 4(b)], near the Si-seed [Fig. 4(c)], and near the edge of the mesh-pattern [Fig. 4(d)]. These results indicate that Ge growth initiated from the (100) Si-seed propagates along the hexagonal-type mesh-pattern while keeping its orientation. This enables the complete (100) crystallization of the entire region (500×250 μm^2). This lateral growth has been confirmed by more than 10 samples. In this way, large-area (500×250 μm^2) single-crystalline (100) GOI networks composed of crossing strips are possible to grow.

In summary, the seeded rapid-melting growth of Ge along a mesh-pattern has been studied on insulating films. Lateral growth propagates 100 μm from the Si-seed along a square-type mesh-pattern. However, polycrystalline Ge gradually forms. The bending of the growth direction is found not to be the reason for the polycrystallization. The latent heat generated at each of the branching positions prolongs the melting-time of the liquid-Ge, which enhances the

probability of random spontaneous nucleation. To decrease the branching-number, a hexagonal-type mesh is substituted for the square mesh. This enables the growth of single-crystalline (100) GOI over the entire mesh region (500×250 μm^2). These c-Ge networks formed on insulating films will be useful for the development of Ge-based advanced devices on the Si platform.

[1] M. Miyao, E. Murakami, H. Etoh, K. Nakagawa, and A. Nishida, J. Cryst. Growth **111**, 912 (1991).

[2] C. H. Lee, T. Nishimura, N. Saido, K. Nagashio, K. Kita, and A. Toriumi, Tech. Dig. - Int. Electron Devices Meet. **2009**, 457.

[3] T. Maeda, K. Ikeda, S. Nakaharai, T. Tezuka, N. Sugiyama, Y. Moriyama, and S. Takagi, IEEE Electron Device Lett. **26**, 102 (2005).

[4] N. Sugiyama, T. Tezuka, T. Mizuno, M. Suzuki, Y. Ishikawa, N. Shibata, and S. Takagi, J. Appl. Phys. **95**, 4007 (2004).

[5] T. Maeda, K. Ikeda, S. Nakaharai, T. Tezuka, N. Sugiyama, Y. Moriyama, and S. Takagi, Thin Solid Films **508**, 346 (2006).

[6] T. Akatsu, C. Deguet, L. Sanchez, F. Allibert, D. Rouchon, T. Signamarcheix, C. Richtarch, A. Boussagol, V. Loup, F. Mazen, J.-M. Hartmann, Y. Campidelli, L. Clavelier, F. Letertre, N. Kernevez, and C. Mazure, Mater. Sci. Semicond. Process. **9**, 444 (2006).

[7] Y. Liu, M. D. Deal, and D. Plummer, Appl. Phys. Lett. **84**, 2563 (2004).

[8] D. J. Tweet, J. J. Lee, J. S. Maa, and S. T. Hsu, Appl. Phys. Lett. **87**, 141908 (2005).

[9] S. Balakumar, M. M. Roy, B. Ramamurthy, C. H. Tung, S. Fei, S. Tripathy, C. Dongzhi, R. Kumar, N. Balasubramanian, and D. L. Kwong, Electrochem. Solid-State Lett. **9**, G158 (2006).

[10] T. Hashimoto, C. Yoshimoto, T. Hosoi, T. Shimura, and H. Watanabe, Appl. Phys. Express **2**, 066502 (2009).

[11] J. Feng, Y. Liu, P. B. Griffin, and J. D. Plummer, IEEE Electron Device Lett. **27**, 911 (2006).

[12] M. Miyao, T. Tanaka, K. Toko, and M. Tanaka, Appl. Phys. Express **2**, 045503 (2009).

[13] K. Toko, T. Tanaka, Y. Ohta, T. Sadoh, and M. Miyao, Appl. Phys. Lett. **97**, 152101 (2010).

[14] M. Miyao, K. Toko, T. Tanaka, and T. Sadoh, Appl. Phys. Lett. **95**, 022115 (2009).

[15] K. Toko, M. Kurosawa, H. Yokoyama, N. Kawabata, T. Sakane, Y. Ohta, T. Tanaka, T. Sadoh, and M. Miyao, Appl. Phys. Express **3**, 075603 (2010).

[16] V. D. Cammilleri, V. Yam, F. Fossard, C. Renard, D. Bouchier, P. F. Fazzini, and M. Hÿtch, J. Appl. Phys. **106**, 093512 (2009).

[17] H. Y. Yu, S. l. Cheng, J. H. Park, A. K. Okyay, M. C. Onbaşlı, B. Ercan, Y. Nishi, and K. C. Saraswat, Appl. Phys. Lett. **97**, 063503 (2010).